Supramolecular Architectures of Streptavidin on Biotinylated Self-Assembled Monolayers. Tracking Biomolecular Reorganization after Bioconjugation

Omar Azzaroni,* Mònica Mir, and Wolfgang Knoll

Max-Planck-Institut für Polymerforschung Ackermannweg 10, 55128 Mainz, Germany

Received: August 21, 2007; In Final Form: October 2, 2007

In this work we have studied the supramolecular bioconjugation of streptavidin (SAv) on biotinylated self-assembled monolayers. By using the quartz crystal microbalance technique with dissipation we were able to follow in real time the biomolecular reorganization within the film. The overall process could be described as an early stage involving a significant increase in surface coverage followed by another stage where the SAv layer slowly reached the asymptotic coverage. Finally, a reorganization process takes place in the bioconjugated film. These results on the kinetics of biomolecular reorganization can be described in terms of the Lifshitz-Slyozov law. These are the first experimental results demonstrating the complexity and the different time scales involved on the bioconjugation of SAv at solid−liquid interfaces. We consider that these findings could have strong implications on the molecular design of biosensing platforms.

Introduction

Immobilization of proteins at solid−liquid interfaces is one of the most challenging topics in the field of biosensing.[1,2] The reason for this increasing interest originates from the wide range of applications of these systems in diagnostics and biotechnology.[3,4] Within the broad family of proteins. streptavidin (SAv) is of particular importance due to its extremely high and very specific interactions[5] with biotin ($K = 10^{15}$ L mol^{-1}) that makes it a most common platform in many biosensors.[6−8]

SAv is a 60 000 Da protein purified from the bacterium *Streptomyces avidinii*. This protein has four binding sites for biotin located on two opposite sides of the tetrameric protein. It can thus be used to link two different functions in the new molecular complex. This means that the protein has unique properties as an adapter for the binding of a second layer of biotinylated molecules.

SAv conjugation on biotinylated platforms has been extensively studied by a number of different research groups.[9−16] That is the case of SAv conjugation on biotinylated lipid bilayers at air−liquid interfaces or at solid−liquid interfaces. The later involved different strategies such as the use of biotin-modified lipid bilayers supported on SiO_2,[17] biotin-functionalized Langmuir-Schaefer binary monolayers,[18] or biotinylated polymer-supported lipid bilayers.[19] Another example is the covalent linking of a carboxymethylated dextran layer with streptavidin, forming carboxylamides. This surface modification was used to attach biotinylated oligonucleotide capture probes to detect the BRCA1 gene.[20]

On the other hand, self-assembled monolayers (SAMs) represent an extremely versatile tool for modifying sensor surfaces and have been accordingly employed for biotin−SAv biorecognition purposes.[21] Detailed studies demonstrated that the choice of the spacer segment of the biotinylated molecule and the dilution of these recognition centers within a hydroxylated matrix play a determinant role on the efficiency of the binding of SAv to the biotin-containing SAM.[22] These studies allowed for the optimization of the specific binding between the SAv and the SAM leading to the widespread use of these supramolecular conjugates as reliable platforms for DNA biosensing.[23,24] Notably, in spite of the tremendous implications on the sensor surface design, the SAv immobilization on biotinylated SAMs has been studied to a much lesser extent.[25−27] Achieving a deep understanding of the mechanisms ruling the formation of the bioconjugated layers and the time scales involved in those processes is of paramount importance in many biotechnological fields, and especially on biosensor design.

It was reported that proteins once adsorbed at the solid−liquid interface can reorganize and change their configuration in order to optimize favorable interactions.[28] However, when dealing with the solid−liquid interface, gaining insight and obtaining reliable information on the biomolecular reconfiguration processes is such a difficult task. That is the reason why so little (or none in the case of SAv) information about these processes is reported in the literature.[29,30] Previous studies were performed by tracking the SAv mass uptake at the solid−liquid interface by following the frequency change or reflectivity changes using a quartz crystal microbalance (QCM) or surface plasmon resonance (SPR), respectively.[31] On the other hand, more information about the same process can be obtained when monitoring the biomolecule immobilization using a quartz crystal microbalance with dissipation (QCM-D). This technique allows for studying the changes in the biomolecular layer through the simultaneous measurements of frequency (f) and dissipation (D).

In the present work we have studied the supramolecular bioconjugation of SAv on biotinylated SAMs using QCM-D. We observed that SAv immobilization proceeds very rapidly as concluded from previous SPR results. However, by following the energy dissipation signal of the microbalance we were able to track in real time the reconfiguration/reorganization of the SAv layer after reaching the asymptotic coverage on the biotinylated platform. Our experiments indicate that, at nearly constant coverage, there are significant structural changes within the biomolecular layer resembling the reported 2D crystallization

* Author to whom correspondence should be addressed. Phone: (+49) 6131-379-357. Fax: (+49) 6131-379-360. E-mail: azzaroni@mpip-mainz.mpg.de.

10.1021/jp076707q CCC: $37.00
Published on Web 11/13/2007

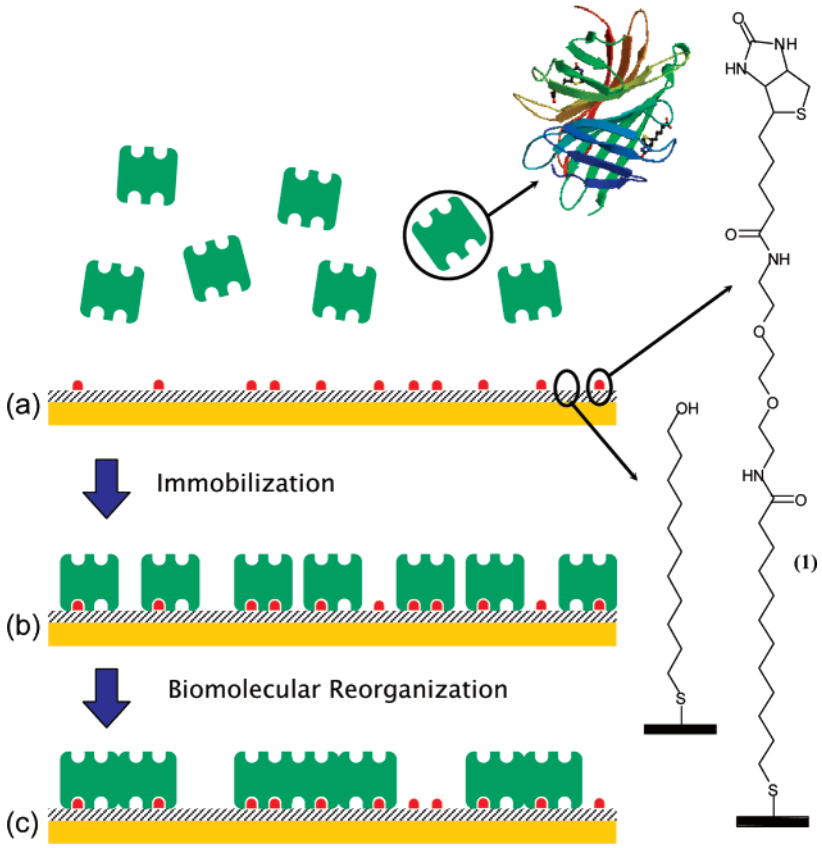

Figure 1. Simplified cartoon describing the supramolecular bioconjugation of streptavidin onto the biotinylated self-assembled monolayer (a), accomplished by an initial immobilization of the protein (b), and followed by its biomolecular reorganization (c).

occurring at the air/water interfaces. Finally, and more important, this protein layer reconfiguration can be interpreted as an Ostwald ripening process (occurring within the bioconjugated film) that can be described in terms of the Lifschitz-Slyozov law. These results are in excellent agreement with previous theoretical predictions based on computational simulations,[32] thus giving for the first time strong experimental evidence about the processes governing the formation of the supramolecular SAv layer.

Experimental Section

Surface plasmon resonance (SPR) detection was carried out in a home-made device under a Kretschmann configuration. The SPR substrates were a BK7 glass coated with 2 nm of chromium and 50 nm of gold evaporated in an Edwards auto 306 cryo. The substrate was incubated overnight with a mixture 1:9 of biotin-terminated thiol and 11-mercapto-1-undecanol. Afterward, the surface was rinsed with ethanol and dried with N_2. Interaction of immobilized biotin and streptavidin was recorded in real-time with SPR. Once a stable baseline is obtained with 100 mM PBS with 0.05% Tween in a flow of 0.992 mL min^{-1}, 1 μM streptavidin in the same buffer and flow rate was injected in the SPR cell. After 1 h of streptavidin incubation, the same buffer was used to rinse the biomolecules that were not interacted with the chip surface. Before and after streptavidin injection, a measure of the SPR signal at different angles was recorded to detect the shift of the minimum angle of refraction due to the streptavidin immobilization on the surface. The SPR angle shifts were converted into mass uptakes using the following experimentally determined relationship: $\Gamma(\text{ng mm}^{-2}) = \Delta\theta(\text{degrees})/0.19$. The sensitivity factor was obtained following procedures reported in the literature.[33]

The QCM-D measurements were carried out at 21 °C using a Q-Sense microbalance (Q-Sense, Göteborg, Sweden). This instrument allows for a simultaneous measurement of frequency change (Δf) and energy dissipation change (ΔD) by periodically switching off the driving power of the oscillation of the sensor crystal and by recording the decay of the damped oscillation. The time constant of the decay is inversely proportional to D, and the period of the decaying signal gives f. Experiments were performed using commercially available (QSX-301, Q-Sense) gold-coated quartz crystals.

Results and Discussion

In our experiments we used a binary mixed SAM chemisorbed on Au surfaces to create the biotinylated surface (Figure 1a). The platform was composed of biotin-terminated thiol (compound **1**) and 11-mercapto-1-undecanol in a 1:9 ratio thus giving the optimum coverage of biotin centers to achieve maximum binding of SAv. These particular conditions are based on experimental evidence reported by Spinke et al.[22] and corroborated by López and co-workers.[26] The optimum configuration refers to biotin centers (isolated biorecognition sites) diluted in a hydroxylated matrix. High coverage of biotin moieties leads to a pronounced decrease of SAv binding, which is attributed to the close packing of biotin groups that hinders the biorecognition with the biotin-binding pocket of SAv.

Figure 2a depicts changes in frequency if a biotinylated gold-coated sensor is in contact with a 1 μM SAv in PBS buffer solution. The initial exposure to the SAv solution leads to a rapid decrease in frequency followed by slight steady decrease before reaching the final plateau.

These frequency changes can be translated into mass coverage in accordance to the Sauerbrey equation:[34]

$$\Delta m = -\frac{C\Delta f}{n} \quad (1)$$

where n is the overtone number, and C is the mass sensitivity constant. In our experimental setup, $C = 17.7$ ng Hz^{-1} cm^{-2}, and we have used different overtones for estimating the mass of the immobilized SAv. Accordingly, the mass uptake associated with the rapid f decrease (in the very early stages) resulted in 495 ng cm^{-2} which slowly increased until reaching a plateau corresponding to 566 ng cm^{-2}.

It is worth noticing that sharp changes in frequency and dissipation should not simply be attributed to the significant increase in mass coverage of bioconjugated SAv. The rapid exchange between solvent and solution can lead to significant changes in frequency and dissipation. In addition, physisorption (nonspecific adsorption) of proteins onto the interfacial bioconjugate can lead to misleading interpretations of the actual frequency and dissipation changes corresponding to the bioconjugation of the protein onto the sensor surface. This is a very important observation that in many cases is not considered in the literature related to the QCM technique.

Reporting frequency changes without properly rinsing the substrate can lead to inconsistent results or even artefacts on the microgravimetric read-out. The strong implications of the nonspecific adsorption on obtaining reliable Δf values have been recently pointed out by Claesson et al.[35] In order to rule out the presence of non-bioconjugated proteins, we proceeded to rinse the sensor with buffer after reaching the late stages of the conjugation (Figure 3). Very slight changes in frequency and dissipation during buffer rinsing corroborate that the detected frequency and dissipation changes could be solely attributed to changes due to protein bioconjugation.

In agreement with the picture described by the QCM, a similar behavior was observed when following the SAv immobilization with SPR (Figure 4). A fast increase followed by a slow increase in reflectivity was observed. In the SPR case, the estimated mass of SAv immobilized corresponded to 210 ng cm^{-2}. This value is in agreement with X-ray photoelectron spectroscopy and near-edge X-ray absorption fine structure measurements on similar biotinylated SAMs reported by Nelson et al. who estimated 230 ng cm^{-2} for SAv coverage.[25]

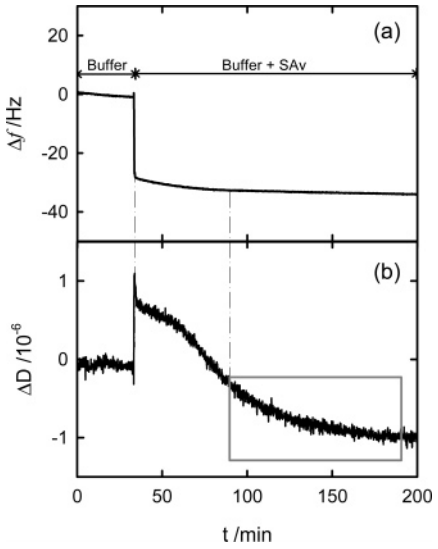

Figure 2. Quartz crystal microbalance response on (a) frequency and (b) dissipation at the overtone number $n = 3$ (15 MHz) when the biotinylated gold-coated quartz crystal is placed in 1 μM SAv solution (in PBS buffer). Frequency changes depicted in the plot correspond to $\Delta f = \Delta f_{15}$ MHz/3.

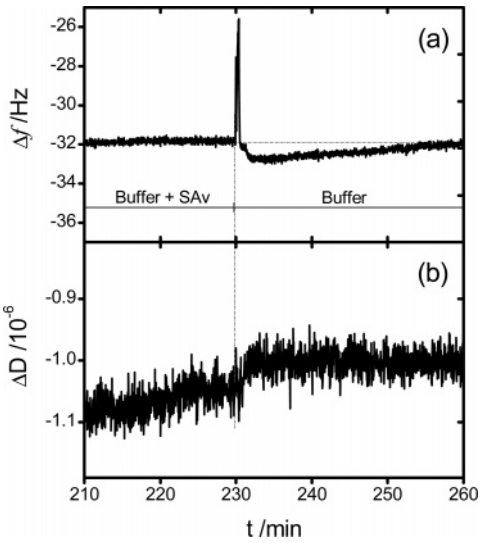

Figure 3. Quartz crystal microbalance response on (a) frequency and (b) dissipation at the first overtone (15 MHz) when the biotinylated gold-coated quartz crystal is rinsed with PBS buffer after reaching the late stages of bioconjugation in 1 μM SAv (in PBS buffer). Frequency changes depicted in the plot correspond to $\Delta f = \Delta f_{15}$ MHz/3. The large spike in frequency is due to a temporary instability in the QCM system when changing solution.

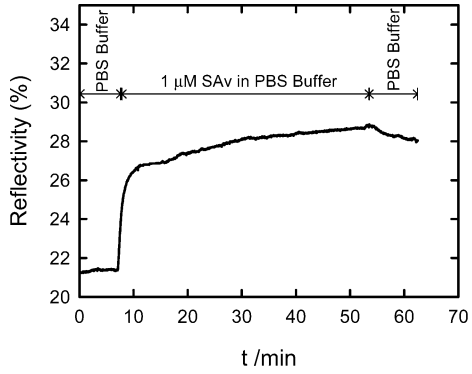

Figure 4. SPR sensorgram corresponding to the immobilization of SAv on the biotinylated platform.

Regarding these differences in mass uptake between Δm_{QCM} and Δm_{SPR}, it must be noted that the QCM-D response is extremely sensitive not only to the viscoelastic properties but also to the density and thickness of any mass coupled to the quartz crystal surface.[29,36] In our case, the film is constituted by SAv molecules conjugated to the biotinylated sensor surface in an aqueous solution. As a consequence, a fraction of solvent is trapped between the adsorbed SAv molecules. More important, this retained water is not strictly "fixed" to the film if we consider that it does not behave as the liquid layer above the film.[17,29,37] In other words, the QCM detects the solvent that is hydrodynamically coupled to the bioconjugated SAv.[17,38] In contrast, the SPR response that originated from refractive index changes as water is replaced by biomolecules, is mostly proportional to the masses of the adsorbed biomolecules.[17,33]

A most interesting feature is evidenced when following the dissipation (D) trace of the microbalance. A sharp increase in D is immediately followed by a slow decrease during the immobilization of SAv. A similar distinctive feature was recently reported by Höök et al. for SAv immobilization on biotinylated lipid bilayers and was associated with SAv 2D crystallization on top of the lipid bilayer.[17]

The D factor is defined as the ratio between the energy dissipated per cycle of oscillation and the total energy stored

in the oscillating system, that is, sensor surface + film. During recent years, there has been an increasing effort on understanding and relating dissipative losses (changes in *D*) to physical processes (interfacial and/or internal friction) occurring at the biomolecular layer.[39] If the immobilized film is rigidly anchored, implying no changes in the coupling between the sensor and liquid environment, no changes of the energy dissipation are detected. On the other hand, *D* may suffer significant changes if the deposited film is not rigidly attached to the oscillating sensor surface. In other words, a soft film attached to the quartz crystal is deformed during the oscillation, which gives a high dissipation, while as a rigid material it gives a low dissipation.[17,29,39]

In the case of the SAv immobilized on the biotinylated SAM, changes in *D* are reflecting structural changes in the film layer upon immobilization. The decreasing *D* indicates that the film is changing its viscoelastic properties from a soft state to a more rigid state.[37] Interestingly, these structural changes occur even after reaching the asymptotic coverage, suggesting that the "stiffening" of the SAv layer is mostly driven by film reorganization.

This would imply that the SAv immobilization process is more complex than a rapid attachment to the biotinylated SAM, as derived solely from frequency and reflectivity changes in QCM or SPR, respectively.

The results obtained with the QCM-D clearly reflect quite unique characteristics of the SAv layer. In most cases, the immobilization of proteins leads to an increase in dissipation.[39] However, in the case of SAv, we observed exactly the opposite trend. Recently, Höök et al. reported a similar observation during the immobilization of SAv on biotinylated lipid bilayers supported on SiO_2. These researchers attributed this particular feature in the dissipation characteristics to the two-dimensional crystallization of the protein on the biotinylated platform. Moreover, they used the slow decrease in *D* as a "fingerprint" for the successful, reliable, and reproducible formation of the 2D SAv layer.[37]

In our case, we observed that the immobilization of SAv on biotinylated SAMs leads to a more pronounced and well-defined decrease of *D*. In agreement with Höök et al., we attribute these changes in *D* to the film reorganization in a scenario resembling the two-dimensional crystallization on the biotinylated SAM.

The full picture of the SAv immobilization could be described as an early stage where there is a significant increase in surface coverage. In less than 3 min, the protein layer reaches 85% of the asymptotic coverage with viscoelastic characteristics that can be attributed to a rather soft dissipative film (Figure 1b). In a more advanced stage (immobilization time <50 min), the bioconjugated SAv film slowly reaches almost full (asymptotic) coverage, showing no significant changes in viscoelastic properties. In the late stages (immobilization time > 50 min) at nearly full coverage, a significant (2D crystallization-like) reorganization of the film takes place, as derived from the sensitive decrease in *D* (Figure 1c).

The quite unique features of the *D* trace are providing valuable information on the kinetics of the reorganization process occurring in the film at the solid−liquid interface. This reorganization after reaching the asymptotic coverage could be driven by SAv−SAv attractive lateral interactions, where Tyr 22 and Thr 20 residues may stabilize the contact regions by hydrogen bonding.[12,40] These "supramolecularly contacted" SAv's are responsible for the stiffening of the biofilm. The increasing size of domains with "contacted" molecules is reflected in a decreasing dissipation. The energetically favorable

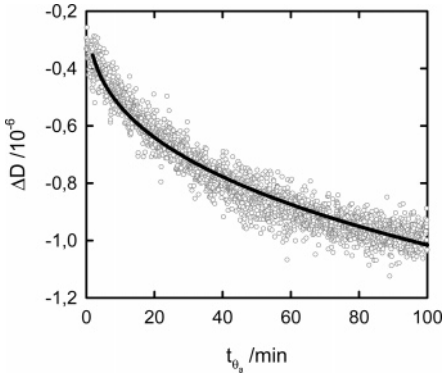

Figure 5. Dissipation trace evidencing viscoelastic changes in the film upon reaching the asymptotic SAv coverage (gray circles). The figure is a detailed zoom of the gray frame in Figure 1. The solid line corresponds to the fitting of the experimental data in accordance to the Lifschitz-Slyozov law (eq 2).

attractive SAv−SAv interactions are the driving force for the growth of "supramolecularly contacted" domains at the expense of noncontacted molecules conjugated to the biotinylated platform. This picture resembles the Ostwald ripening commonly encountered in many physical and chemical systems.[41−44] Regarding this issue, very recently Zhdanov et al. reported on the SAv 2D crystallization studied by Monte Carlo simulations.[32] This group described the growth of SAv crystalline domains as a case of island growth in a preadsorbed layer at fixed adsorbate coverage. They found that the size of the crystalline domains/islands (*R*) grew according to the Lifshitz-Slyozov law,[45] $R \sim t^{1/3}$. However, no experimental evidence has been reported in order to support or verify the proposed mechanism, so far. In our experimental scenario, the overall size of the "contacted" domains is proportional to ΔD. Under this approach, we can write the Lifshitz-Slyozov equation in terms of *D*,

$$D(t) \approx A + Bt^x \tag{2}$$

where *A* and *B* are constants, and *x* is the growth exponent. Figure 4 shows in detail changes in *D* after the SAv reached the asymptotic coverage (gray frame in Figure 1).

Our interest is focused on a phenomenon occurring after the SAv layer is formed, so we re-scaled the time axis in order to describe the reordering as a process starting after reaching the asymptotic coverage. This is analogous to the assumption made by Zhdanov et al. in their Monte Carlo simulations where SAv is rapidly adsorbed at $t = 0$ with no further adsorption.[32] So, the time-resolved process described in Figure 5 and the previously reported Monte Carlo simulations have similar and comparable initial conditions. From fitting the *D* versus *t* plot (Figure 5) with eq 2, we obtained the following results: $A = -0.117$, $B = -0.19$, and $x = 0.335$. The value of the growth exponent strongly supports previous computational results suggesting a reorganization process following an Ostwald ripening or Lifshitz-Slyozov-type kinetics. As far as we know, this is the first experimental evidence demonstrating the reordering processes occurring at SAv layers bioconjugated on biotinylated SAMs.

Conclusions

Our work was focused on studying the supramolecular bioconjugation of SAv on biotinylated SAMs. These studies indicate that the SAv immobilization process is more complex than a simple rapid attachment to the biotinylated SAM, as commonly derived by QCM or SPR studies. The overall process

could be described as an early stage involving a significant increase in surface coverage driven mostly by the high affinity between the surface-confined biotin species and biotin-binding pockets in the SAv molecules. The molecular recognition between ligand and receptor leads to a rapid immobilization/conjugation of the biomolecule on the functionalized surface. This initial process is followed by another stage where the SAv layer slowly reaches the asymptotic coverage. This process would probably involve further bioconjugation of SAv on vacant sites on the SAv layer initially conjugated. Finally, after reaching asymptotic coverage, reorganization of the SAv layer takes place. This process promotes a gradual stiffening of the biomolecular film as evidenced by the pronounced change in the viscoelastic properties. By analyzing the changes in dissipation, we were able to follow in real time the biomolecular reorganization within the film. Our results on the kinetics of biomolecular reorganization are in excellent agreement with previously reported Monte Carlo simulations. These results indicate that the reorganization is an Ostwald ripening-type process that can be asymptotically described by the Lifshitz-Slyozov law. To the best of our knowledge, these are the first experimental results demonstrating the complexity and the different time scales involved in the bioconjugation of SAv at solid−liquid interfaces. We think that these results could be relevant in different areas of biotechnology, with special emphasis on the research community devoted to biosensing.

Acknowledgment. O.A. acknowledges financial support from the Alexander von Humboldt Stiftung.

References and Notes

(1) Mayes, A. G. In *Biomolecular Sensors*; Gizeli, E., Lowe, C. R., Eds.; Taylor & Francis: London, 2002; Chapter 4, pp 49−86.
(2) Dubrovsky, T. B. In *Protein Architecture: Interfacing Molecular Architecture and Immobilization Biotechnology*; Lvov, Y., Möhwald, H., Eds.; Marcel Dekker: New York, 2000; Chapter 2, pp 25−54.
(3) Palecek, E.; Fojta, M. In *Bioelectronics: From Theory to Applications*; Katz, E., Willner, I., Eds.; VCH-Wiley: Weinheim, 2005; Chapter 5, pp 127−192.
(4) Bashir R. In *Encyclopedia of Nanoscience, Engineering and Technology*; Goddard, W. A., III, Brenner, D. W., Lyshevski, S. E., Iafrate, G. J., Eds.; CRC Press: Boca Raton, 2003; Chapter 15, pp 15-1//15-28.
(5) Weber, P. C.; Ohlendorf, D. H.; Wendoloski, J. J.; Salemme, F. R. *Science* **1989**, *243*, 85−88.
(6) Smith, C. L.; Milea, J. S.; Nguyen, G. H. *Top. Curr. Chem*. **2006**, *261*, 63−90.
(7) Bonanno, L. M.; DeLouise, L. A. *Langmuir* **2007**, *23*, 5817−5823.
(8) Stayton, P. S.; Nelson, K. E.; McDevitt, T. C.; Edwards, T.; Castner, D. G.; Shimoboji, T.; Ding, Z.; Hoffman A. In *Protein Architecture: Interfacing Molecular Assemblies and Immobilization Technology*; Lvov, Y., Möhwald, H., Eds.; Marcel Dekker: New York, 2000; Chapter 11, pp 287−310.
(9) Dietrich, J.; Vénien-Bryan, C. *Strategies for Two-Dimensional Crystallization of Proteins Using Lipid Monolayers*; Imperial College Press: London, 2005.
(10) Blankenburg, R.; Meller, P.; Ringsdorf, H.; Salesse, C. *Biochemistry* **1989**, *28*, 8214−8221.
(11) Reviakine, I.; Brisson, A. *Langmuir* **2001**, *17*, 8293−8299.
(12) Koppenol, S.; Klumb, L. A.; Vogel, V.; Stayton, P. S. *Langmuir* **1999**, *14*, 7125−7129.
(13) Yatcilla, M. T.; Robertson, C. R.; Gast, A. P. *Langmuir* **1998**, *14*, 497−503.
(14) Wang, S.-W.; Robertson, C.; Gast, A.; Koppenol, S.; Edwards, T.; Vogel, V.; Stayton, P. *Langmuir* **2000**, *16*, 5199−5204.
(15) Schief, W. R.; Edwards, T.; Frey, W.; Koppenol, S.; Stayton, P. S.; Vogel, V. *Biomol. Eng.* **1999**, *16*, 29−38.
(16) Darst, S. E.; Ahlers, M.; Meller, P. H.; Kubalek, E. W.; Blankenburg, R.; Ribi, H. O.; Ringsdorf, H.; Kornberg, R. D. *Biophys. J.* **1991**, *59*, 387−396.
(17) Larsson, C.; Rodahl, M.; Höök, F. *Anal. Chem*. **2003**, *75*, 5080−5087.
(18) Ihalainen, P.; Peltonen, J. *Sens. Actuators B: Chem*. **2004**, *102*, 207−218.
(19) Calvert, T. L.; Leckband, D. *Langmuir* **1997**, *13*, 6737−6745.
(20) Gronewold, T. M. A.; Baumgarten, A.; Quandt, E.; Famulok, M. *Anal. Chem*. **2006**, *78*, 4865−4871.
(21) Häussling, L.; Ringsdorf, H.; Schmitt, F. J.; Knoll, W. *Langmuir* **1991**, *7*, 1837−1840.
(22) Spinke, J.; Liley, M.; Schmitt, F.-J.; Guder, H.-J.; Angermaier, L.; Knoll, W. *J. Chem. Phys.* **1993**, *99*, 7012−7019.
(23) Sabanayagam, C. R.; Smith, C. L.; Cantor, C. R. *Nucleic Acid Res.* **2000**, *28*, e33.
(24) Liu, J.; Tian, S.; Tiefenauer, L.; Nielsen, P. E.; Knoll, W. *Anal. Chem.* **2005**, *77*, 2756−2761.
(25) Nelson, K. E.; Gamble, L.; Jung, L. S.; Boeckl, M. S.; Naeemi, E.; Gollegde, S. L.; Sasaki, T.; Castner, D. G.; Campbell, C. T.; Stayton, P. S. *Langmuir* **2001**, *17*, 2807−2816.
(26) Pérez-Luna, V. H.; O'Brien, M. J.; Opperman, K. A.; Hampton, P. D.; López, G. P.; Klumb, L. A.; Stayton, P. S. *J. Am. Chem. Soc.* **1999**, *121*, 6469−6478.
(27) Häussling, L.; Michel, B.; Ringsdorf, H.; Rohrer, H. *Angew. Chem., Int. Ed.* **1991**, *30*, 569−572.
(28) Norde, W. In *Physical Chemistry of Biological Interfaces*; Baszkin, A., Norde, W., Eds.; Marcel Dekker: New York, 2000; Chapter 4, pp 115−135.
(29) Höök, F.; Rodahl, M.; Brzezinski, P.; Kasemo, B. *J. Colloid Interface Sci.* **1998**, *208*, 63−67.
(30) Höök, F.; Rodahl, M.; Kasemo, B.; Brezezinski, P. *Proc. Natl. Acad. Sci. U.S.A.* **1998**, *95*, 12271−12276.
(31) Su, X.; Wu, Y.-J.; Robelek, R.; Knoll, W. *Langmuir* **2005**, *21*, 348−353.
(32) Zhdanov, V. P.; Höök, F.; Kasemo, B. *Proteins* **2001**, *43*, 489−498.
(33) Stenberg, E.; Persson, B.; Roos, H.; Urbaniczky, C. *J. Colloid Interface Sci.* **1991**, *143*, 513−526.
(34) Sauerbrey, G. *Z. Phys.* **1959**, *155*, 206−222.
(35) Kaufman, E. D.; Belyea, J.; Johnson, M. C.; Nicholson, Z. M.; Ricks, J. L.; Shah, P. K.; Bayless, M.; Pettersson, T.; Feldoto, Z.; Blomberg, E.; Claesson, P.; Franzen, S. *Langmuir* **2007**, *23*, 6053−6062.
(36) Höök, F.; Rodahl, M.; Brzezinski, P.; Kasemo, B. *Langmuir* **1998**, *14*, 729−734.
(37) Höök, F.; Ray, A.; Nordén, B.; Kasemo, B. *Langmuir* **2001**, *17*, 8305−8312.
(38) Rodahl, M.; Dahlqvist, P.; Höök, F.; Kasemo, B. In *Biomolecular Sensors*; Gizeli, E., Lowe, C. R., Eds.; Taylor & Francis: London, 2002; Chapter 12, pp 304−316.
(39) Rodahl, M.; Höök, F.; Fredriksson, C.; Keller, C. A.; Krozer, A.; Brzezinski, P.; Voinova, M.; Kasemo, B. *Faraday Discuss.* **1997**, *107*, 229−246.
(40) Coussaert, T.; Völkel, A. R.; Noolandi, J.; Gast, A. P. *Biophys. J.* **2001**, *80*, 2004−2010.
(41) Morgenstern, K.; Rosenfeld, G.; Comsa, G. *Phys. Rev. Lett*. **1996**, *76*, 2113−2116.
(42) Hausser, F.; Voigt, A. *Phys. Rev. B* **2005**, *72*, 035437-1/11
(43) Zhdanov, V. P. *Eur. Phy. J. B* **2001**, *19*, 97−100.
(44) Zhdanov, V. P. *Surf. Sci*. **1997**, *392*, 185−198.
(45) Lifshitz, I. M.; Slyozov, V. V. *J. Phys. Chem. Solids* **1961**, *19*, 35−50.